

Dalton Transactions

An international journal of inorganic chemistry

Accepted Manuscript

This article can be cited before page numbers have been issued, to do this please use: T. Keles, Z. Byklolu, G. Seyhan and B. Barut, *Dalton Trans.*, 2026, DOI: 10.1039/D6DT00405A.



This is an Accepted Manuscript, which has been through the Royal Society of Chemistry peer review process and has been accepted for publication.

Accepted Manuscripts are published online shortly after acceptance, before technical editing, formatting and proof reading. Using this free service, authors can make their results available to the community, in citable form, before we publish the edited article. We will replace this Accepted Manuscript with the edited and formatted Advance Article as soon as it is available.

You can find more information about Accepted Manuscripts in the [Information for Authors](#).

Please note that technical editing may introduce minor changes to the text and/or graphics, which may alter content. The journal's standard [Terms & Conditions](#) and the [Ethical guidelines](#) still apply. In no event shall the Royal Society of Chemistry be held responsible for any errors or omissions in this Accepted Manuscript or any consequences arising from the use of any information it contains.

Structure–Activity Relationships of Morpholine-Modified Silicon(IV) Phthalocyanines as Potential Antidiabetic Agents

View Article Online
DOI: 10.1039/D6DT00405A

Turgut Keleş^{a,b}, Zekeriya Biyiklioglu^{c*}, Gökçe Seyhan^{d,e}, Burak Barut^d

^aKaradeniz Technical University, Graduate School of Natural and Applied Science, Trabzon, Türkiye

^bCentral Research Laboratory Application and Research Center, Recep Tayyip Erdogan University, Rize, Turkey

^cKaradeniz Technical University, Faculty of Science, Department of Chemistry, Trabzon, Türkiye

^dKaradeniz Technical University, Faculty of Pharmacy, Department of Biochemistry, Trabzon, Türkiye

^eKaradeniz Technical University, Graduate School of Health Sciences, Department of Biochemistry (Pharmacy), Trabzon, Türkiye

Corresponding author; Tel: +90 462 377 36 64, Fax: +90 462 325 31 96

E-mail addresses: zekeriya@ktu.edu.tr (Z. Biyiklioglu)



Abstract

View Article Online
DOI: 10.1039/D6DT00405A

Type 2 diabetes mellitus (DM) is a chronic metabolic disorder with a rapidly increasing global prevalence, highlighting the need for safer and more effective therapeutic strategies. In this study, a series of axially disubstituted silicon(IV) phthalocyanines bearing morpholine functional groups and their water-soluble derivatives were synthesized, structurally characterized, and evaluated for their antidiabetic potential. The synthesized compounds were characterized by FT-IR, ^1H and ^{13}C NMR, UV-Vis spectroscopy, and mass spectrometry. The *in vitro* antidiabetic activity of the compounds was evaluated through α -glycosidase and α -amylase inhibition assays. The non-ionic silicon(IV) phthalocyanine derivatives MT-C3-H-Si and MT-C3-D-Si exhibited strong α -glucosidase inhibitory activity with IC_{50} values of $16.02 \pm 0.94 \mu\text{M}$ and $44.14 \pm 4.06 \mu\text{M}$, respectively, showing higher potency than the standard inhibitor acarbose ($\text{IC}_{50} = 60.51 \pm 4.66 \mu\text{M}$). In contrast, the water-soluble derivatives MT-C3-H-SiQ and MT-C3-D-SiQ displayed lower inhibitory activity ($\text{IC}_{50} = 68.80 \pm 5.12 \mu\text{M}$ and $>100 \mu\text{M}$, respectively), indicating that increased hydrophilicity does not necessarily enhance enzyme inhibition. All compounds exhibited weak α -amylase inhibition ($\text{IC}_{50} >100 \mu\text{M}$) compared with acarbose ($\text{IC}_{50} = 25.29 \pm 3.50 \mu\text{M}$). Kinetic studies revealed that MT-C3-H-Si and MT-C3-D-Si inhibit α -glycosidase via a non-competitive mechanism, with K_i values of $9.45 \pm 1.45 \mu\text{M}$ and $29.06 \pm 5.16 \mu\text{M}$, respectively. This is characterized by decreased V_{max} values without significant changes in K_m , suggesting interaction with allosteric regions of the enzyme. Overall, these findings highlight axially disubstituted silicon(IV) phthalocyanines as promising molecular scaffolds and contribute valuable insight into the limited literature on their antidiabetic enzyme inhibition properties.



1. Introduction

Diabetes Mellitus (DM) is a multifactorial metabolic disease characterized by chronic hyperglycemia. Hyperglycemia occurs when the secretion or action of insulin is deficient. Due to their relationship with insulin, DM affects adipose tissues, skeletal muscles, and the liver. In diabetic patients, it presents with symptoms such as increased polyphagia, polydipsia, polyuria, weight loss, and visual impairment^{1,2}. If left untreated, the disease progresses and may lead to severe complications including blindness, cardiovascular disease, stroke, and renal dysfunction³. According to the International Diabetes Federation shows that in 2021, approximately 540 million adults had DM, which is projected to reach approximately 640 million in 2030 and 790 million in 2045. Therefore, health expenditures for this disease are quite high. Health expenditures, which were \$966 billion in 2021, are expected to reach \$1054 billion in 2045⁴. DM is a major global health concern, and although there is no definitive cure, it can be effectively managed. Blood glucose levels can be controlled through insulin therapy, pharmacological agents, and lifestyle modifications, including diet and physical activity. Type 1 and Type 2 DM are the most common types of DM⁵. Among these, Type 2 DM accounts for approximately 90% of all cases, is characterized by impaired insulin secretion due to pancreatic β -cells dysfunction and decreased insulin sensitivity resulting from abnormalities in insulin receptors⁶. One of the key therapeutic strategies for managing Type 2 DM involves the inhibition of carbohydrate-digesting enzymes. In this context, α -glycosidase and α -amylase enzymes have attracted considerable attention as important targets in drug development. α -glycosidase plays a critical role in the hydrolysis of α -(1,6)-D-glycosidic bonds, facilitating the breakdown of complex carbohydrates into absorbable monosaccharides. Inhibition of this enzyme helps regulate postprandial hyperglycemia without directly affecting insulin secretion⁷. Similarly, α -amylase catalyzes the hydrolysis of α -(1,4)-D-glycosidic bonds, contributing to starch digestion⁸. Clinically used inhibitors such as acarbose, miglitol, and voglibose are effective; however, there are often associated with gastrointestinal side effect, including flatulence, abdominal discomfort, and bloating. These adverse effects are primarily attributed to the strong inhibition of α -amylase and α -glycosidase, leading to the fermentation of undigested carbohydrates^{9,10}. Therefore, the development of novel inhibitors with strong α -glycosidase inhibition and mild provide enhanced efficacy, minimal adverse effects, and strong α -glycosidase and mild α -amylase inhibition remains an important research objective.

In the mid-twentieth century, significant progress was made in the development of new macroheterocyclic compounds through the incorporation of different elements into the



phthalocyanines core ¹¹.

View Article Online
DOI: 10.1039/D6DT00405A

Like closely related porphyrin analogues, phthalocyanines have an 18 π -electron conjugated system. However, unlike porphyrins, they contain imine bridges and isoindole units instead of methine bridges and pyrrole rings ¹². These structural differences result in strong absorption in the red and near-infrared (NIR) region, typically 700 nm ¹³. Despite these advantageous optical properties, the application of phthalocyanines is often limited by their poor solubility and strong tendency to aggregate due to π - π stacking interactions ¹⁴. To overcome these limitations, various structural modifications strategies have been developed, including the introduction of substituents and metal ions into the macrocyclic core to improve solubility, reduce aggregation, and enhance synthetic accessibility ¹⁵. Among metal phthalocyanines, silicon(IV) phthalocyanines have attracted particular interest due to their unique hexacoordinated structure and remarkable stability of Si-N bonds ¹⁶. Additionally, the presence of two unique axial positions that can be easily functionalized provides a significant advantage over conventional phthalocyanines. Bulky or polar substituents introduced at these axial positions are more effective than α - or β -substituted phthalocyanines, as they disrupt intermolecular interactions and reduce planarity¹⁷. In additions, axial Si-O and Si-C bonds have enabled a wide range of applications in biomedical fields due to their stability, cost-effective synthesis, and low toxicity¹⁸. Especially in biological systems, silicon(IV) phthalocyanines exhibit improved performance compared to peripheral and non-peripheral metal phthalocyanines, as axial ligands increase the distance between macrocycles, thereby reducing aggregation and intermolecular interactions¹⁹.

Furthermore, water-soluble silicon(IV) phthalocyanines can be readily obtained via simple quaternization of nitrogen atoms in axially substituted groups with methyl iodide. These ionic derivatives are considered promising candidates for biological applications, particularly as enzyme inhibitors in metabolic diseases. Several studies have investigated the biological activity of silicon(IV) phthalocyanines. For examples, Solgun et al. synthesized axially disubstituted bis-(3,4,5-trimethoxybenzyloxy)silicon(IV) phthalocyanine. The antidiabetic activity of the compound was investigated at concentrations of 100, 200 and 400 mg/L and 22.66%, 29.16% and 41.66% enzyme inhibition was recorded, respectively²⁰. In another study, Çelik et al. investigated the α -amylase and α -glucosidase enzyme inhibition activities of silicon(IV) phthalocyanines (6a and 6b) containing 1,2,3-triazole Schiff base groups²¹. Compound 6a showed very little inhibition against α -amylase, while it did not inhibit α -glucosidase. However, 6b showed moderate inhibition against α -amylase, while α -glucosidase showed about 8 times more effective inhibition compared to acarbose. The presence of electron-



releasing methoxy groups in compound 6b may have increased the activity. In a similar study, Yalazan et al. designed axially disubstituted silicon(IV) phthalocyanines with geraniol and phytol groups, which are acyclic hydrocarbons. The α -glycosidase inhibitory effects of silicon(IV) phthalocyanines were tested using spectrophotometric assays. These compounds had lower α -glycosidase inhibition activity compared to acarbose²². Overall, studies on the α -glycosidase and α -amylase enzyme inhibition activities of silicon(IV) phthalocyanines remain limited, highlighting the need for further investigation in this area.

Therefore, one of the aims of this study was to design and develop new silicon(IV) phthalocyanines and investigate their activities against these enzymes. On the other hand, the potential of these new silicon(IV) phthalocyanine compounds as drug candidates for the treatment of DM has been evaluated.

In this study, axially disubstituted silicon(IV) phthalocyanines containing morpholine groups and their water-soluble derivatives were synthesized and characterized using NMR, FT-IR, UV-Vis and MS spectroscopic techniques. Afterwards, the α -glycosidase and α -amylase enzyme inhibition activities of these compounds were investigated. Inhibition activities, kinetic tests, inhibition types and inhibition constants of these compounds were reported in detail.

2. Material and methods

All solvents and reagents used in the reactions were of reagent grade quality and were obtained from commercial suppliers. Also, the materials, equipments, *in vitro* α -glycosidase and α -amylase inhibition assay, kinetic and statistical analysis experiments were presented in data SI.

2.1. The synthesis of 4-(3-(3-chloropropoxy)phenyl)morpholine (MT-C3-Cl)

In a 250 mL double-necked flask, 1 g (5.60 mmol) of 3-(4-morphonyl)phenol and 200 mg (8.40 mmol) of NaH in 10 mL of dry DMF were stirred at 0 °C to -5 °C under a nitrogen gas atmosphere for 1 hour. To this mixture, 0.60 mL (5.60 mmol) of 1-bromo-3-chloropropane in 3 mL dry DMF was slowly added using a dropping funnel. The reaction mixture was stirred at room temperature under a nitrogen gas atmosphere for 1 day. At the end of the time, the contents of the flask were poured into an ice-water mixture, 50 mL of chloroform was added and the reaction mixture was stirred for 1 day. The crude product was then extracted 3 times with a chloroform/water mixture. The chloroform was then evaporated under reduced pressure and the crude product was purified from the column loaded with aluminum oxide, using chloroform as



mobile phase. Yield: 650 mg (46 %). IR (ATR), $\bar{\nu}_{\max}/\text{cm}^{-1}$: 3095–3031 (Ar–H), 2962–2824 (Alif. C–H), 1600, 1496, 1450, 1382, 1304, 1257, 1192, 1122, 1051, 993, 877, 835, 759, 687, 651. ¹H-NMR (DMSO-*d*₆), (δ:ppm): 7.10 (t, 1H, Ar–H), 6.52 (d, 1H, Ar–H), 6.45 (s, 1H, Ar–H), 6.40 (d, 1H, Ar–H), 4.03 (t, 2H, Ar–O–CH₂), 3.76 (t, 2H, CH₂–Cl), 3.70 (t, 4H, CH₂–O), 3.06 (t, 4H, CH₂–N), 2.15–2.09 (m, 2H, –CH₂–). ¹³C-NMR (DMSO-*d*₆), (δ:ppm): 159.75, 152.91, 130.11, 108.35, 105.35, 102.23, 66.52, 64.42, 48.82, 42.47, 32.24. LC/MS (ESI) *m/z*: 256.210 [M]⁺.

2.2. The synthesis of (4-(3-(3-morpholine)phenoxy)propoxy)phenyl)methanol (MT-C3-H-OH)

In a 250 mL flask, 315 mg (2.53 mmol) 4-hydroxybenzyl alcohol and 2.4 g (17.70 mmol) dry K₂CO₃ were dissolved in 60 mL acetone. To the reaction mixture was added 650 mg (2.53 mmol) 4-(3-(3-(3-chloropropoxy)phenyl)morpholine (MT-C3-Cl) and 528 mg (2 mmol) 18-crown-6 and stirred at 70 °C under nitrogen atmosphere for 2 days. The reaction was cooled to room temperature, filtered through black band filter paper and the solvent was evaporated. The crude product obtained was extracted 3 times with a chloroform/water mixture. The solvent of the organic phase was completely evaporated and the crude product was purified with chloroform through a neutral silica gel-loaded column. Yield: 380 mg (44 %), melting point: 85–87 °C. IR (ATR), $\bar{\nu}_{\max}/\text{cm}^{-1}$: 3426 (–OH), 3051 (Ar. C–H), 2967–2837 (Alif. C–H), 1614, 1576, 1512, 1448, 1393, 1301, 1266, 1240, 1196, 1113, 1042, 963, 876, 837, 745, 680. ¹H-NMR (DMSO-*d*₆), (δ:ppm): 7.21 (d, 2H, Ar–H), 7.09 (t, 1H, Ar–H), 6.89 (d, 2H, Ar–H), 6.51 (d, 1H, Ar–H), 6.45 (s, 1H, Ar–H), 6.40 (d, 2H, Ar–H), 4.39 (s, 2H, CH₂–OH), 4.08 (t, 4H, Ar–O–CH₂), 3.70 (t, 4H, CH₂–O), 3.06 (t, 4H, CH₂–N), 2.13–2.10 (m, 2H, –CH₂–). ¹³C-NMR (DMSO-*d*₆), (δ:ppm): 159.88, 157.80, 152.87, 135.04, 130.10, 128.34, 114.48, 108.27, 105.47, 102.24, 66.51, 64.61, 64.43, 62.97, 48.85, 29.20. LC/MS (ESI) *m/z*: 344.310 [M+H]⁺.

2.3. The synthesis of (3,5-bis(3-(3-morpholinophenoxy)propoxy)phenyl)methanol (MT-C3-D-OH)

MT-C3-D-OH was synthesized similarly to the synthesis of MT-C3-H-OH. 3,5-dihydroxy benzyl alcohol was used instead of 4-hydroxybenzyl alcohol. Yield: 400 mg (55 %). IR (ATR), $\bar{\nu}_{\max}/\text{cm}^{-1}$: 3437 (–OH), 3092–3035 (Ar–H), 2963–2830 (Alif. C–H), 1598, 1497, 1450, 1383, 1266, 1193, 1163, 1119, 1066, 996, 834, 760, 688. ¹H-NMR (DMSO-*d*₆), (δ:ppm): 7.09 (t, 2H, Ar-H), 6.48 (t, 6H, Ar-H), 6.37 (t, 3H, Ar-H), 4.39 (s, 2H, CH₂–OH), 4.06 (t, 8H, Ar–O–CH₂),



3.68 (t, 8H, CH₂-O), 3.05 (t, 8H, CH₂-N), 2.11-2.08 (m, 4H, -CH₂-). ¹³C-NMR (DMSO-d₆) (δ:ppm): 159.97, 159.87, 152.90, 145.64, 130.09, 108.25, 105.42, 105.09, 102.19, 99.86, 66.51, 64.60, 64.39, 63.22, 48.83, 29.17. MALDI-TOF-MS m/z: 578.038 [M]⁺.

2.4. The synthesis of silicon(IV) phthalocyanine compound (MT-C3-H-Si)

In a 50 mL flask, 120 mg (0.35mmol) of (4-(4-(3-(3-morpholinphenoxy)propoxy)phenyl)phenyl)methanol (MT-C3-H-OH) was dissolved in 10 mL of dry toluene and 100 mg (0.16 mmol) of silicon phthalocyanine dichloride was added and stirred under nitrogen atmosphere for 10 minutes. Then 8.40 mg (0.35 mmol) sodium hydride was added to the reaction medium and the mixture was stirred at 110 °C for one day. At the end of the time, the mixture was cooled to room temperature and the solvent was removed by evaporation. The crude product was purified from the neutral silica gel loaded column using chloroform as mobile phase. Yield: 45 mg (18%), m.p: >250 °C. IR (ATR), $\bar{\nu}_{\max}/\text{cm}^{-1}$: 3069 (Ar-H), 2964–2855 (Alif. C-H), 1600, 1507, 1429, 1335, 1291, 1242, 1193, 1167, 1121, 1077, 908, 759, 731, 680. ¹H-NMR (CDCl₃), (δ:ppm): 9.58 (m, 8H, Pc-H_α), 8.31 (m, 8H, Pc-H_β), 7.14 (t, 4H, Ar-H), 6.51 (d, 4H, Ar-H), 6.40 (s, 4H, Ar-H), 5.68 (d, 4H, Ar-H), 4.24 (t, 4H, -Ar-O-CH₂)_b, 3.96 (s, 4H, Ar-O-CH₂)_d, 3.81 (t, 8H, CH₂-O)_f, 3.11 (t, 8H, CH₂-N)_e, 2.00 (m, 4H, -CH₂-)_c, -0.78 (s, 4H, Si-O-CH₂)_a. ¹³C-NMR (CDCl₃), (δ:ppm): 159.87, 156.17, 152.65, 149.28, 136.03, 131.29, 130.68, 129.81, 124.59, 123.55, 112.55, 108.46, 105.35, 102.63, 66.85, 64.30, 63.98, 57.42, 49.24, 29.10. UV-Vis (DMF) λ_{\max} nm (log ε): 678 (5.04), 650 (4.29), 612 (4.33), 332 (4.66). MALDI-TOF-MS m/z: 1225.105 [M]⁺.

2.5. The synthesis of silicon(IV) phthalocyanine compound (MT-C3-D-Si)

The synthesis of MT-C3-D-Si phthalocyanine was synthesized similarly to MT-C3-H-Si phthalocyanine with minor modification, using the compound (3,5-bis(3-(3-morpholinphenoxy)propoxy)phenyl)phenyl)methanol (MT-C3-D-OH) instead of MT-C3-H-OH. The crude product was purified from the neutral silica gel loaded column using chloroform as mobile phase. Yield: 60 mg (22%), m.p: >250 °C. IR (ATR), $\bar{\nu}_{\max}/\text{cm}^{-1}$: 3081(Ar-H), 2960-2860 (Alif. C-H), 1597, 1496, 1450, 1336, 1260, 1192, 1162, 1121, 1066, 996, 832, 757, 738, 688. ¹H-NMR (CDCl₃), (δ:ppm): 9.57 (m, 8H, Pc-H_α), 8.27 (m, 8H, Pc-H_β), 7.18 (t, 6H, Ar-H), 6.53 (d, 6H, Ar-H), 6.43 (t, 8H, Ar-H), 5.50 (s, 2H, Ar-H), 3.85 (t, 8H, Ar-O-CH₂)_b, 3.83(d, 16H, CH₂-O)_f, 3.17 (t, 8H, Ar-O-CH₂)_d, 3.12 (t, 16H, CH₂-N)_e, 1.84 (m, 8H, -CH₂-)_c, -0.72



(s, 4H, Si–O–CH₂)_a. ¹³C-NMR (CDCl₃), (δ:ppm): 159.87, 158.27, 152.66, 149.37, 141.45, 135.99, 130.78, 129.82, 123.54, 108.46, 105.45, 102.68, 101.21, 99.20, 66.86, 64.34, 63.42, 58.16, 49.28, 29.05. UV-Vis (DMF) λ_{max} nm (log ε): 681 (5.00), 648 (4.26), 615 (4.30), 335 (4.65). MALDI-TOF-MS m/z: 1695.166 [M]⁺.

2.6. The general synthesis of water-soluble silicon(IV) phthalocyanines

20 mg (0.016 mmol) MT-C3-H-Si and MT-C3-D-Si were dissolved separately in 2.50 mL of chloroform and 2 mL of iodomethane was added to these mixtures. The reaction mixtures were stirred at room temperature in the dark for 6 days. At the end of the time, the precipitated part was filtered through a glass crucible. The unreacted portion was washed with chloroform and diethylether and removed from the medium. The obtained portion was dried in vacuo.

2.6.1. The synthesis of MT-C3-H-SiQ

Yield: 15 mg (61%), m.p.: >300 °C. IR (ATR), $\bar{\nu}_{\max}/\text{cm}^{-1}$: 3056 (Ar–H), 2932–2807 (Alif. C–H), 1612, 1519, 1469, 1429, 1337, 1290, 1166, 1119, 1067, 911, 830, 759, 727. UV-Vis (DMF) λ_{max} nm (log ε): 668 (5.04), 643 (4.63), 604 (4.35), 355 (4.88). MALDI-TOF-MS m/z: 682.570 [M-2I+3H₂O+H]²⁺.

2.6.2. The synthesis of MT-C3-D-SiQ

Yield: 10 mg (38%), m.p.: >300 °C. IR (ATR), $\bar{\nu}_{\max}/\text{cm}^{-1}$: 3060 (Ar–H), 2985–2881 (Alif. C–H), 1610, 1519, 1471, 1425, 1332, 1287, 1167, 1119, 1064, 910, 832, 757, 729. UV-Vis (DMF) λ_{max} nm (log ε): 668 (5.03), 643 (4.33), 604 (4.35), 355 (4.60). MALDI-TOF-MS m/z: 440.849 [M-4I+H]⁴⁺.

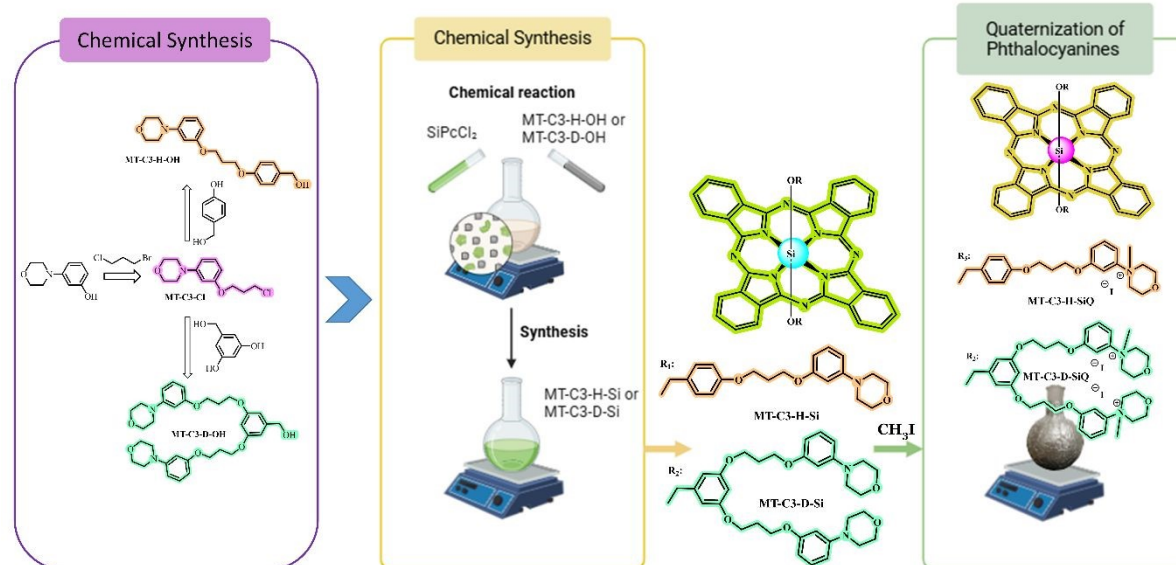
3. Results and Discussion

3.1. Synthesis and characterization

Scheme 1 illustrates the synthetic route for morpholine-substituted silicon(IV) phthalocyanines (MT-C3-H-Si and MT-C3-D-Si) and their water-soluble derivatives (MT-C3-H-SiQ and MT-C3-D-SiQ). Initially, the compound MT-C3-Cl was synthesized via a nucleophilic substitution reaction between 3-morpholine phenol and 1-bromo-3-chloropropane in DMF using NaH as a



base.

View Article Online
DOI: 10.1039/D6DT00405A

Scheme 1. Synthetic route for the preparation of axially disubstituted silicon(IV) phthalocyanines (MT-C3-H-Si and MT-C3-D-Si) and their water-soluble derivatives (MT-C3-H-SiQ and MT-C3-D-SiQ).

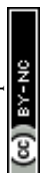
The synthesized ligand precursor MT-C3-Cl was characterized by FT-IR, NMR, and ESI-MS techniques to confirm its molecular structure. In the IR spectrum of MT-C3-Cl, aromatic C–H stretching vibrations were observed at 3095–3031 cm^{-1} , while aliphatic C–H stretching bands appeared at 2962–2824 cm^{-1} , indicating the presence of both aromatic and aliphatic moieties in the molecule. The characteristic aromatic C=C stretching band was detected at 1600 cm^{-1} , supporting the presence of the aromatic ring system. In addition, the C–O–C and C–N–C stretching vibrations observed at 1257 and 1122 cm^{-1} , respectively, are characteristic of the morpholine ring and confirm the presence of the ether and tertiary amine functionalities associated with the morpholine moiety in the proposed structure (Fig. S1). The ^1H NMR spectrum (DMSO- d_6) of MT-C3-Cl exhibited four aromatic protons in the range of 7.10–6.40 ppm, which correspond to the protons on the substituted aromatic ring. The fourteen aliphatic protons observed between 4.03 and 2.15 ppm are attributed to the methylene groups associated with the morpholine and propyl fragments (Fig. S2a). In the ^{13}C NMR spectrum, aromatic carbon signals were observed in the range of 159.75–102.23 ppm, while aliphatic carbons appeared at 66.52 ($\text{CH}_2\text{--O}$), 64.42 (Ar--O--CH_2), 48.82 ($\text{CH}_2\text{--N}$), 42.47 ($\text{CH}_2\text{--Cl}$), and 32.24 ppm ($\text{--CH}_2\text{--}$), supporting the structural integrity of the compound (Fig. S2b). Notably, the signal at 42.47 ppm is characteristic of a C–Cl carbon environment, whereas C–Br carbons are typically observed at lower chemical shift values (ca. 30–40 ppm). This observation indicates



that the substitution occurred via bromide displacement, resulting in the formation of the chlorine-containing product, in agreement with literature reports^{23,24}. The ESI-MS spectrum further supports the proposed structure, showing a molecular ion peak at $m/z = 256.21$ corresponding to the protonated molecule $M+H^+$ (Fig. S3). In addition, a signal at $m/z = 298.21$ was detected and carefully evaluated. Detailed inspection of the magnified spectrum revealed that this peak does not exhibit the characteristic isotopic pattern of bromine ($M/M+2$ doublet with approximately 1:1 intensity for $^{79}\text{Br}/^{81}\text{Br}$)²⁵. Therefore, the presence of a brominated species can be excluded. Instead, this signal is attributed to a solvent-derived adduct, most likely, which is commonly observed in ESI-MS analyses. Subsequently, MT-C3-H-OH and MT-C3-D-OH were synthesized via nucleophilic substitution of MT-C3-Cl with 4-hydroxybenzyl alcohol and 3,5-dihydroxybenzyl alcohol, respectively, in acetone using K_2CO_3 as a base. This reaction pathway enables the introduction of hydroxybenzyl substituents through a nucleophilic displacement of the chlorine atom, leading to the formation of ether-linked derivatives.

The IR spectra of both MT-C3-H-OH and MT-C3-D-OH confirmed the successful substitution reaction. In particular, the appearance of broad O–H stretching bands at 3426 cm^{-1} for MT-C3-H-OH and 3437 cm^{-1} for MT-C3-D-OH clearly indicates the presence of hydroxyl groups in the molecular structures. Aromatic C–H stretching bands were observed at 3051 cm^{-1} for MT-C3-H-OH and $3092\text{--}3035\text{ cm}^{-1}$ for MT-C3-D-OH, while aliphatic C–H stretching vibrations appeared in the ranges of $2967\text{--}2837\text{ cm}^{-1}$ and $2963\text{--}2830\text{ cm}^{-1}$, respectively, which are consistent with the coexistence of aromatic and aliphatic fragments within the ligands (Fig. S4 and S7). The ^1H NMR spectrum of MT-C3-H-OH ($\text{DMSO-}d_6$) displayed aromatic proton signals between 7.21 and 6.40 ppm and aliphatic proton signals between 4.39 and 2.10 ppm, which are consistent with the expected proton environments of the substituted benzyl, morpholine and alkyl units (Fig. S5a). The ^{13}C NMR spectrum showed sixteen carbon signals within the range of 159.88–29.20 ppm, confirming the presence of both aromatic and aliphatic carbon atoms in the structure (Fig. S5b). Similarly, the ^1H NMR spectrum of MT-C3-D-OH exhibited aromatic proton signals in the range of 7.09–6.37 ppm and aliphatic proton signals between 4.39 and 2.11 ppm (Fig. S8a). The ^{13}C NMR spectrum displayed sixteen carbon signals between 159.97 and 29.17 ppm, which is consistent with the proposed molecular framework containing aromatic rings and aliphatic chains (Fig. S8b).

The mass spectra further confirmed the molecular structures of the synthesized ligands. The molecular ion peak was observed at $m/z\ 344.310\ [M+H]^+$ for MT-C3-H-OH (Fig. S6) and at

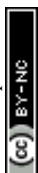


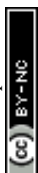
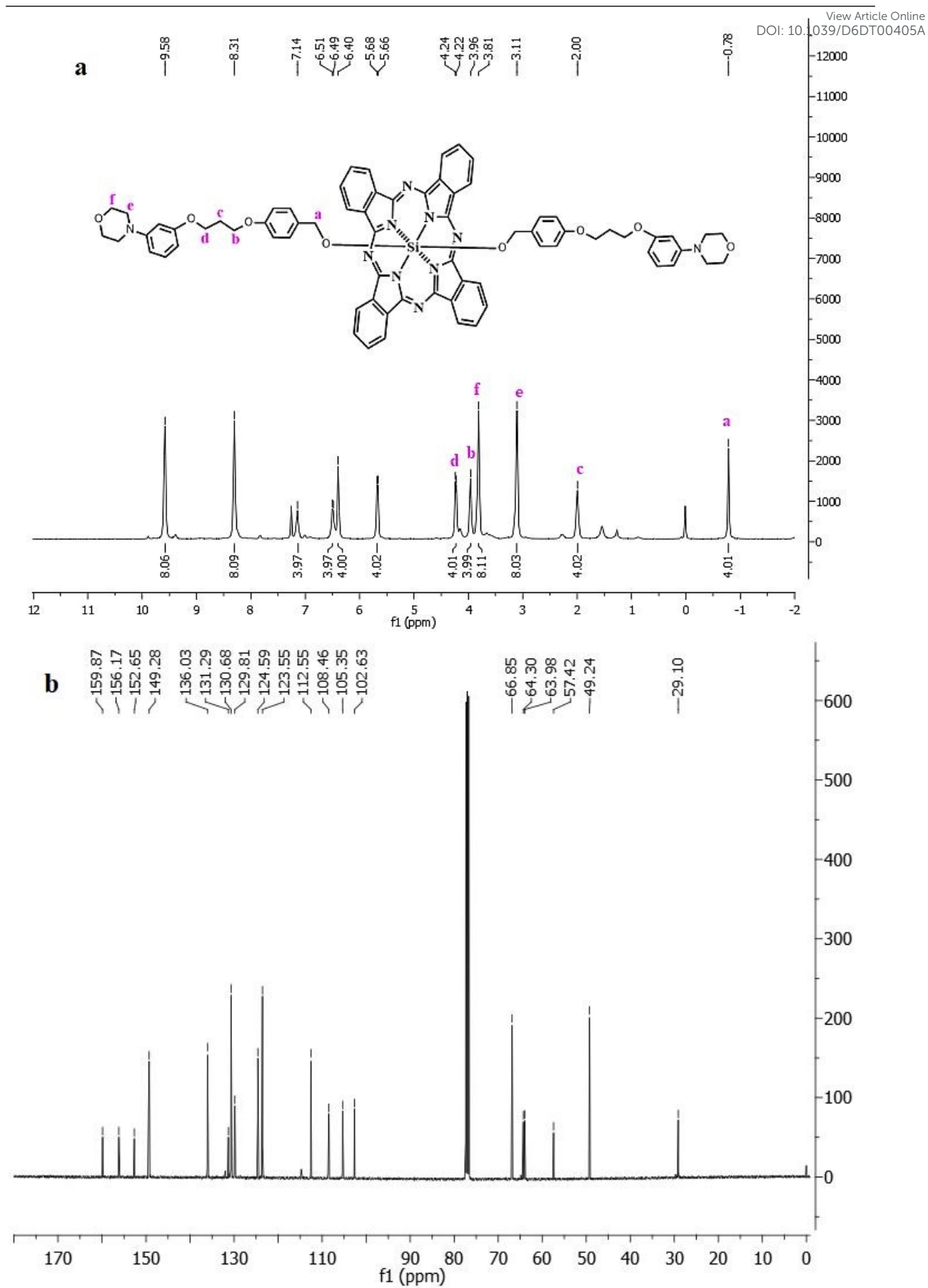
m/z 578.038 $[M]^+$ for MT-C3-D-OH (Fig. S9), which are consistent with their expected molecular weights and verify the formation of the target compounds.

The silicon(IV) phthalocyanines MT-C3-H-Si and MT-C3-D-Si were obtained by reacting the corresponding hydroxyl derivatives with NaH and SiPcCl₂ in toluene at 110 °C for 24 h. In the FT-IR spectra, the disappearance of O–H stretching bands confirmed axial substitution. Aromatic C–H stretching vibrations were observed at 3069 cm⁻¹ for MT-C3-H-Si and 3081 cm⁻¹ for MT-C3-D-Si, while aliphatic C–H stretching bands appeared at 2964–2855 cm⁻¹ and 2960–2860 cm⁻¹, respectively (Fig.S10 and S11).

The ¹H NMR spectrum (CDCl₃) of MT-C3-H-Si exhibited characteristic phthalocyanine macrocycle proton signals. The Pc-H_α and Pc-H_β protons appeared at 9.58 and 8.31 ppm, respectively, which are typical for silicon(IV) phthalocyanine derivatives and confirm the presence of the phthalocyanine core. Additional aromatic proton signals were observed between 7.14 and 5.68 ppm, corresponding to the benzyl aromatic rings introduced through axial substitution, while the aliphatic proton signals resonated in the range of 4.24–2.00 ppm, originating from the morpholine and propyl fragments.

Notably, the Si–O–CH₂ protons were detected at –0.78 ppm. This unusual upfield shift can be attributed to the strong magnetic anisotropy of the phthalocyanine macrocycle, where the ring current effect of the conjugated π-system generates a shielding environment above and below the macrocyclic plane, causing the axial substituent protons located in this region to resonate at negative chemical shift values. This observation further supports the successful axial coordination of the substituents to the silicon center²⁶ (Fig. 1a). The ¹³C NMR spectrum displayed aromatic carbon signals between 159.87 and 102.63 ppm, which are attributed to the carbon atoms of the phthalocyanine macrocycle and the aromatic benzyl substituents. In addition, aliphatic carbon signals were observed between 66.85 and 29.10 ppm, corresponding to the carbons of the morpholine and propyl groups introduced through axial substitution (Fig. 1b).





Similarly, MT-C3-D-Si exhibited characteristic phthalocyanine macrocycle proton signals, where Pc-H_α and Pc-H_β resonances appeared at 9.57 and 8.27 ppm, respectively. These signals are typical for silicon(IV) phthalocyanine derivatives and confirm the integrity of the phthalocyanine core. Additional aromatic proton signals were observed between 7.18 and 5.50 ppm, corresponding to the aromatic benzyl units attached through axial substitution, while the aliphatic proton signals appearing at 3.85–1.84 ppm were attributed to the morpholine groups and propyl fragments. Similar to the MT-C3-H-Si derivative, the Si–O–CH₂ protons were observed at -0.72 ppm due to the strong magnetic anisotropy and ring current effects of the phthalocyanine macrocycle, which create a shielding environment for the axial substituent protons (Fig. 2a). The ¹³C NMR spectrum revealed fourteen aromatic carbon signals in the range of 159.87–99.20 ppm, corresponding to the carbon atoms of the phthalocyanine macrocycle and the aromatic substituents. In addition, six aliphatic carbon signals were observed between 66.86 and 29.05 ppm, which are assigned to the carbons of the morpholine and propyl chains, further supporting the presence of the axial substituents in the synthesized silicon(IV) phthalocyanine structure (Fig. 2b).

View Article Online
DOI: 10.1039/D6DT00405A



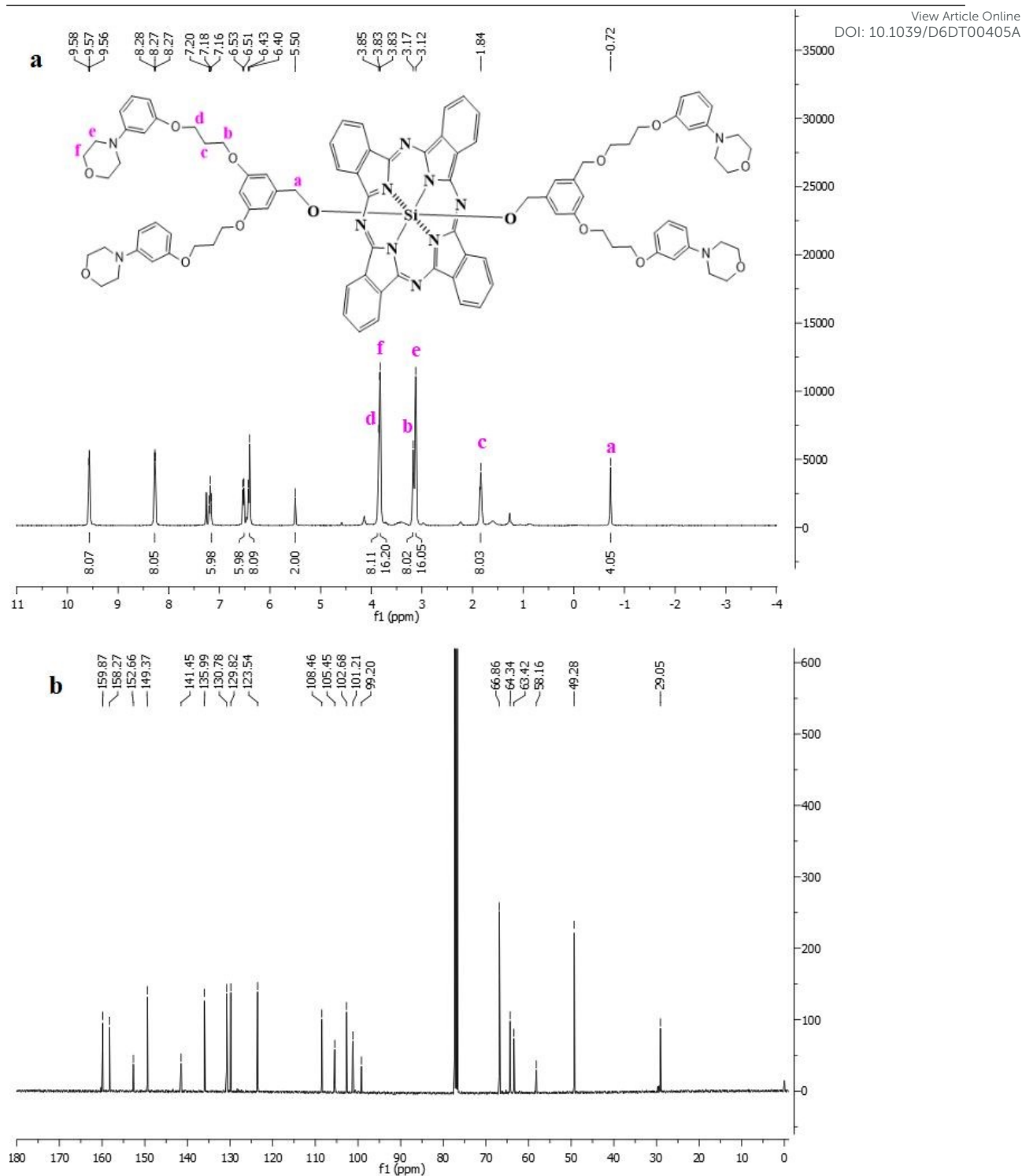


Figure 2. ^1H NMR (a) and ^{13}C NMR (b) spectra of MT-C3-D-Si recorded in CDCl_3 .

MALDI-TOF MS analysis showed molecular ion peaks at m/z 1225.105 $[\text{M}]^+$ for MT-C3-H-Si and 1695.166 $[\text{M}]^+$ for MT-C3-D-Si (Fig. 3). These molecular ion signals are consistent with the expected molecular weights of the target silicon(IV) phthalocyanine derivatives and provide further confirmation of the axial substitution and formation of the proposed structures.



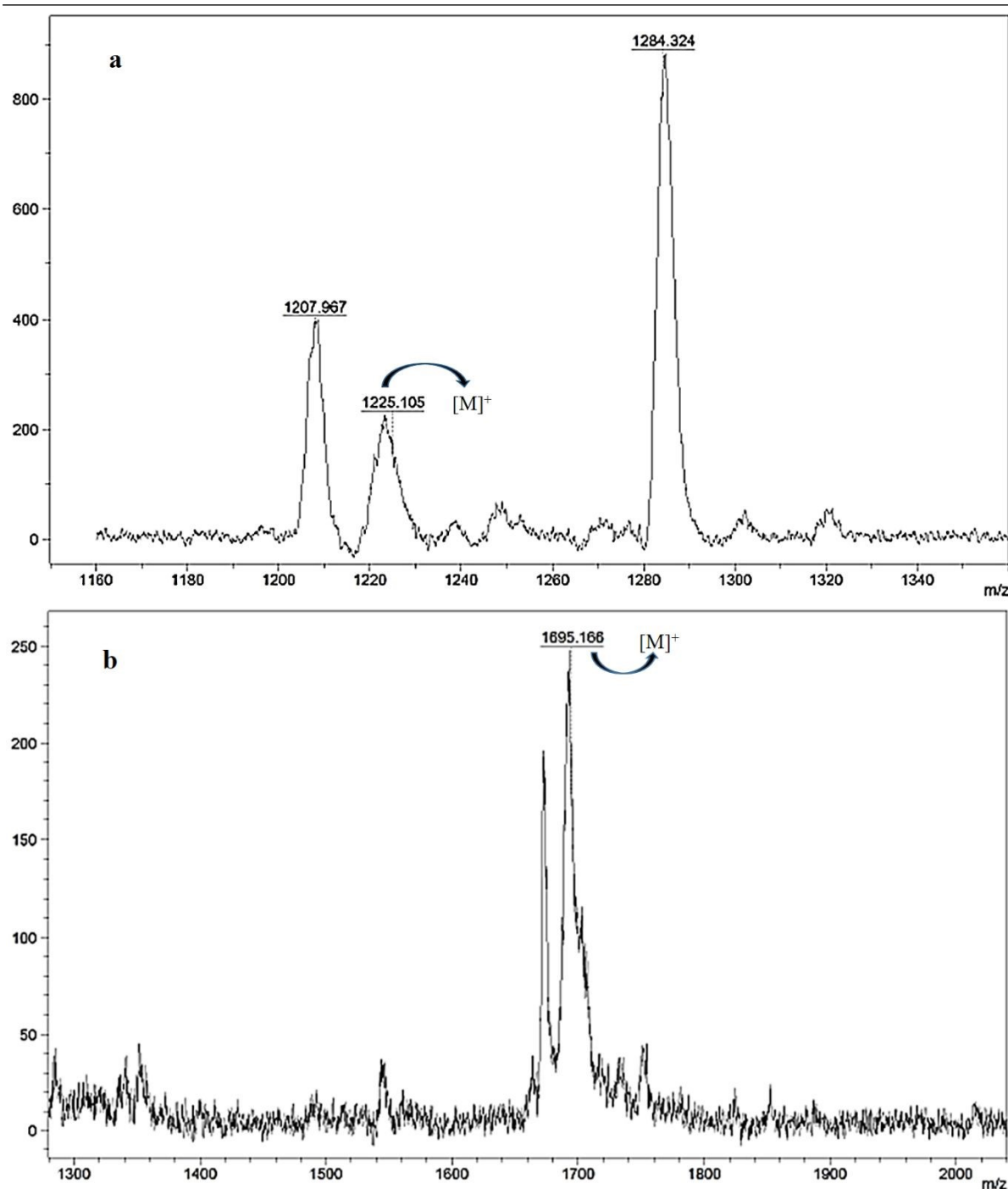


Figure 3. MALDI-TOF MS spectrum of MT-C3-H-Si (a) and MT-C3-D-Si (b).

UV-Vis spectra recorded in DMF indicated that both phthalocyanines predominantly exist in a non-aggregated (monomeric) form, displaying characteristic Q bands at 678 nm for MT-C3-H-Si and 681 nm for MT-C3-D-Si, together with B (Soret) bands at 332 and 335 nm, respectively (Fig. 4). The presence of sharp and well-defined Q bands suggests that axial substitution with morpholine-containing ligands effectively suppresses π - π stacking interactions between



phthalocyanine macrocycles in DMF, thereby reducing aggregation behavior.

View Article Online
DOI: 10.1039/D6DT00405A

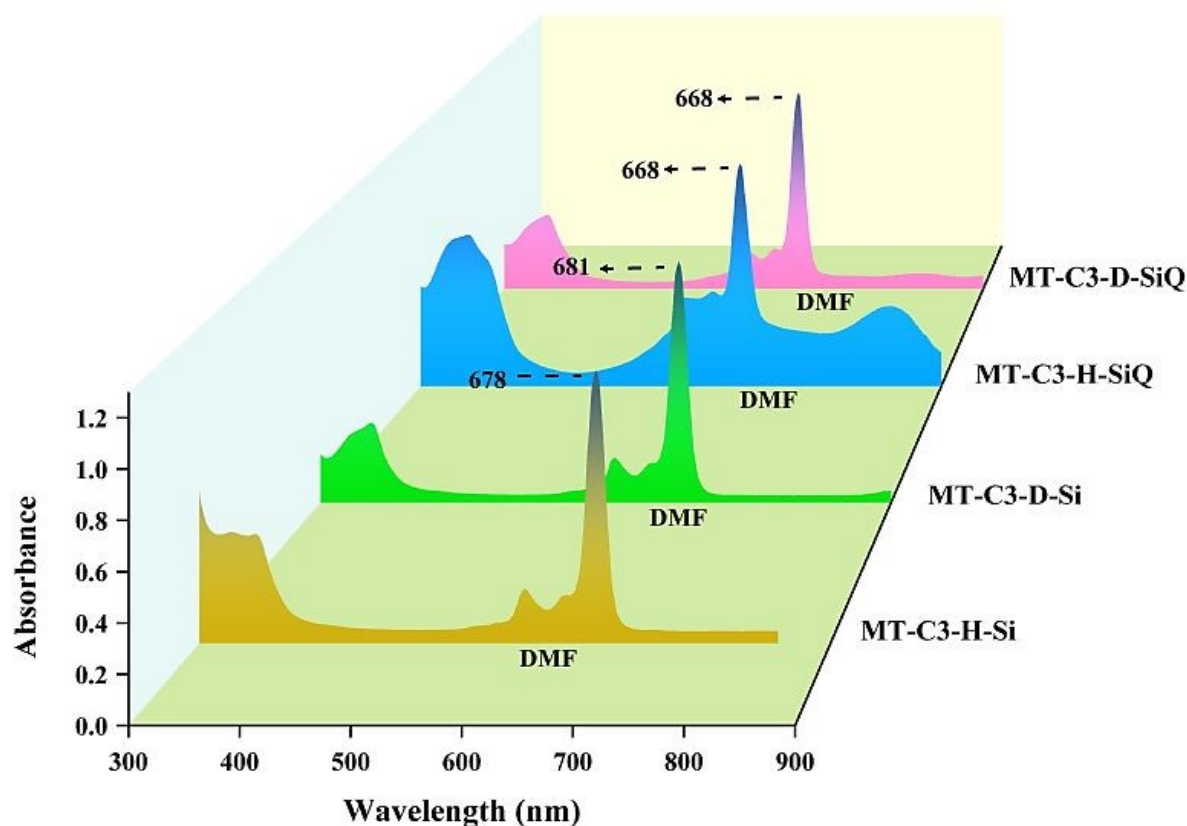


Figure 4. UV–Vis absorption spectrum of silicon(IV) phthalocyanines recorded in DMF.

Finally, the water-soluble derivatives MT-C3-H-SiQ and MT-C3-D-SiQ were synthesized by quaternization of MT-C3-H-Si and MT-C3-D-Si with iodomethane in chloroform at room temperature. This quaternization reaction converts the tertiary amine groups into quaternary ammonium salts, thereby introducing ionic character and enhancing the solubility of the silicon(IV) phthalocyanine derivatives in polar media. The FT-IR spectra of the quaternized compounds were generally similar to those of their non-ionic counterparts, indicating that the phthalocyanine macrocycle and axial substituent framework remained structurally intact after the quaternization process (Fig. S12 and S13). In the UV–Vis spectra recorded in DMF, both MT-C3-H-SiQ and MT-C3-D-SiQ displayed characteristic Q and B bands at 668 nm and 355 nm, respectively (Fig. 4). Compared with the non-quaternized silicon(IV) phthalocyanines, the water-soluble derivatives exhibited a noticeable shift in the Q-band region, which can be attributed to the electronic influence of the introduced ionic substituents and the resulting changes in the electronic environment of the phthalocyanine macrocycle. In contrast, partial aggregation was observed for the water-soluble derivative MT-C3-H-SiQ under the same



solvent conditions. This behavior may arise from increased intermolecular interactions associated with the ionic substituents, which can promote aggregation despite the steric effects of axial substitution^{27,28}.

The water-soluble derivatives were characterized by MALDI-TOF mass spectrometry using dithranol (DIT) and 3-indoleacrylic acid (IAA) as matrices. For MT-C3-H-SiQ, the expected molecular ion was not observed; instead, signals at lower m/z values (356.563, 556.514, 682.570, 881.249, and 912.496) were detected, which are attributed to fragment ions formed after iodide loss. In particular, the peak at m/z 682.570 can be assigned to the $[M-2I+3H_2O+H]^{2+}$ species, indicating the loss of iodide ions followed by hydration (Fig. 5a). This behavior is consistent with the known ionization characteristics of quaternary ammonium salts under MALDI conditions. For MT-C3-D-SiQ, a prominent peak at m/z 440.849 was observed and assigned to the $M-4I+H^{4+}$ species, supporting the formation of the tetracationic framework. Additional signals at m/z 557.495, 577.397, 594.448, and 609.730 were attributed to lower charge states and/or partially fragmented species (Fig. 5b). The overall spectral features, including iodide loss, multiply charged ions, and fragmentation patterns, are consistent with the proposed quaternary structures.

View Article Online
DOI: 10.1039/D6DT00405A



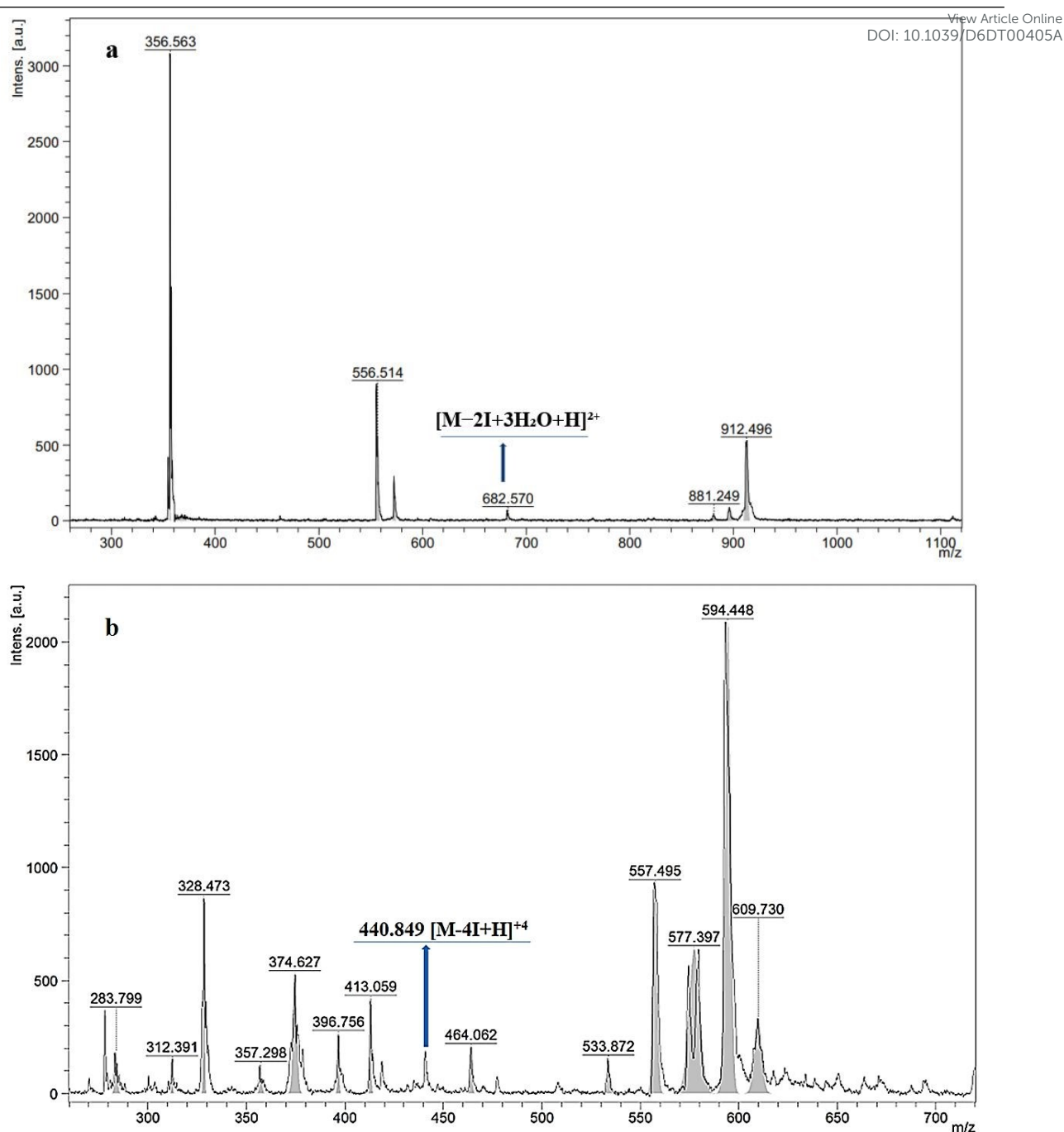


Figure 5. MALDI-TOF MS spectrum of MT-C3-H-SiQ (a) and MT-C3-D-SiQ (b).

3.2. Assays for enzyme inhibition

The α -glycosidase and α -amylase inhibitory activities of the synthesized compounds were evaluated, and the results are summarized in Table 1. Based on the α -glycosidase inhibition data, MT-C3-H-Si exhibited the highest inhibitory activity with an IC_{50} value of 16.02 ± 0.94 μ M, followed by MT-C3-D-Si with an IC_{50} value of 44.14 ± 4.06 μ M. The water-soluble derivatives MT-C3-H-SiQ and MT-C3-D-SiQ showed lower inhibitory activities, with IC_{50}



values of $68.80 \pm 5.12 \mu\text{M}$ and $>100 \mu\text{M}$, respectively. The standard inhibitor acarbose displayed an IC_{50} value of $60.51 \pm 4.66 \mu\text{M}$. Notably, MT-C3-H-Si and MT-C3-D-Si demonstrated significantly higher inhibitory activity than acarbose ($p < 0.0001$).

Table 1. The α -glycosidase and α -amylase inhibitory properties of compounds.

| Compounds | α -Glycosidase (μM) | α -Amylase (μM) |
|-------------|---|-------------------------------------|
| MT-C3-H-Si | $16.02 \pm 0.94^{***}$ | >100 |
| MT-C3-D-Si | $44.14 \pm 4.06^{***}$ | >100 |
| MT-C3-H-SiQ | 68.80 ± 5.12 | >100 |
| MT-C3-D-SiQ | >100 | >100 |
| Acarbose | 60.51 ± 4.66 | 25.29 ± 3.50 |

*** $p < 0.0001$ vs acarbose

Comparable inhibition trends have been reported in the literature. Çelik et al. investigated the α -glycosidase inhibitory activity of silicon(IV) phthalocyanines containing 1,2,3-triazole Schiff base or methoxy homolog substituents and reported that the methoxy-substituted phthalocyanine was approximately 700 times more effective than the standard inhibitor, with an IC_{50} value of $22.4 \pm 1.0 \mu\text{M}$ ²¹. Similarly, Barut and Demirbaş evaluated non-peripheral triclosan-substituted metal-free, copper(II), and nickel(II) phthalocyanines and found that the copper(II) derivative exhibited strong α -glycosidase inhibition ($\text{IC}_{50} = 25.12 \pm 0.62 \mu\text{M}$), surpassing both the other compounds and the standard inhibitor²⁹.

In another study, Khan et al. synthesized benzimidazolium salts bearing N-methylmorpholine groups and reported α -glycosidase IC_{50} values ranging from 15 ± 0.03 to $110 \pm 0.11 \mu\text{M}$, with the bromo-substituted derivative identified as the most potent inhibitor ($\text{IC}_{50} = 15 \pm 0.03 \mu\text{M}$)³⁰. Menteşe et al. reported even stronger inhibition for certain morpholine derivatives, with IC_{50} values between 0.18 ± 0.021 and $20.46 \pm 0.21 \mu\text{M}$, and a 4-methoxyphenyl-substituted compound showing approximately 900-fold higher inhibition than the standard inhibitor³¹. Çakmak et al. investigated morpholine-substituted quinoline derivatives and reported IC_{50} values between 584.20 ± 62.51 and $1023.16 \pm 103.27 \mu\text{M}$, which were still higher than that of the standard inhibitor ($\text{IC}_{50} = 1160.7 \pm 172 \mu\text{M}$), with the 5-nitro-3,6,8-tribromoquinoline derivative exhibiting the highest inhibition³².

Within the present study, MT-C3-H-Si and MT-C3-D-Si emerged as the most active silicon(IV) phthalocyanines in terms of α -glycosidase inhibition. The presence of morpholine substituents



appears to contribute positively to α -glycosidase inhibition, consistent with previously reported structure–activity relationships. However, literature reports focusing specifically on α -glycosidase inhibition by silicon(IV) phthalocyanines remain limited, and the results of the present study are in agreement with the available findings. Several studies have demonstrated the effectiveness of morpholin-derived compounds as scaffold structures for developing in vitro antidiabetic agents³³. Kayukova and colleagues tested the enzyme inhibitory potential of aroil-(morpholin-1-yl)propionamidoxime bases and their salts. These compounds inhibited α -glycosidase by 22.8% to 78.7% and α -amylase by 25.6% to 48.0%. They exhibited α -glycosidase inhibitory effects comparable to acarbose, while demonstrating weak α -amylase inhibition³⁴. In a different study, Saroha and co-workers examined the in vitro amylase inhibitory activity of morpholine-conjugated aurone derivatives. It was found that these compounds exhibited moderate inhibition of α -amylase, ranging from 7.22% to 22.48%³⁵.

Regarding α -amylase inhibition, all synthesized compounds exhibited IC_{50} values above 100 μM , indicating weak inhibitory activity, whereas the standard inhibitor acarbose showed an IC_{50} value of $25.29 \pm 3.50 \mu M$. This inhibition profile is consistent with the desired pharmacological behavior for Type II diabetes management, where selective α -glycosidase inhibition over α -amylase inhibition is preferred. In a study by Çelik et al., silicon(IV) phthalocyanines displayed IC_{50} values of 78 ± 2 and $>400 \mu M$ against α -amylase, while acarbose showed an IC_{50} value of $48 \pm 2 \mu M$, confirming their weak α -amylase inhibition²¹. Similarly, Saka et al. reported low α -amylase inhibition for peripheral copper(II) and zinc(II) phthalocyanines, with IC_{50} values >450 and $128.2 \pm 1.5 \mu M$, respectively, compared to the standard inhibitor ($IC_{50} = 6.9 \pm 0.1 \mu M$)³⁶.

Additional studies further support this trend. Huneif et al. investigated a vanillin–thiazolidinedione–morpholine hybrid compound and reported IC_{50} values of $10.32 \pm 1.02 \mu M$ for the standard inhibitor and $19.51 \pm 1.34 \mu M$ for the synthesized compound, indicating lower potency relative to the standard³⁷. Likewise, Askarzade et al. demonstrated that a morpholine-containing phthalimide–benzenesulfonamide derivative showed no α -amylase inhibition at 300 μM , whereas acarbose exhibited an IC_{50} value of $108 \pm 0.71 \mu M$ ³⁸.

The water-soluble silicon(IV) phthalocyanines (MT-C3-H-SiQ and MT-C3-D-SiQ) displayed lower inhibitory activity against both α -glycosidase and α -amylase compared to their non-ionic counterparts (MT-C3-H-Si and MT-C3-D-Si). This observation suggests that increased hydrophilicity and quaternization may adversely affect enzyme–inhibitor interactions. Enhanced water solubility does not necessarily translate into improved enzyme inhibition, highlighting the importance of maintaining an optimal balance between aqueous solubility and



biological activity during inhibitor design. The fact that the *in vitro* α -amylase inhibitory activity of morpholine derivatives remains at a low to moderate level highlights the need for structural modifications to enhance their efficacy. On the other hand, studies investigating the antidiabetic potential of morpholine-substituted phthalocyanine compounds are quite limited in the literature. Notably, investigations focusing on axially disubstituted and water-soluble silicon(IV) phthalocyanines remain scarce. Therefore, this work provides valuable insight by systematically evaluating both α -glycosidase and α -amylase inhibition, supported by kinetic analysis, within a single silicon(IV) phthalocyanine framework, thereby contributing to an existing gap in the literature.

3.3. Kinetic analyses of compounds

The inhibition mechanism and inhibition constants (K_i) of MT-C3-H-Si and MT-C3-D-Si, which exhibited the highest inhibitory activity against α -glucosidase, were investigated through enzyme kinetic analysis. The kinetic parameters obtained are summarized in Table 2.

Table 2. Kinetic analyses of **MT-C3-H-Si** and **MT-C3-D-Si** on α -glucosidase.

| Compounds | Type | K_i (μM) |
|-------------------|-----------------|-------------------------|
| MT-C3-H-Si | non-competitive | 9.45 ± 1.45 |
| MT-C3-D-Si | non-competitive | 29.06 ± 5.16 |

As shown in Fig. 6, the presence of MT-C3-H-Si led to a decrease in the V_{max} value, while the K_m value remained unchanged. This kinetic behavior indicates that MT-C3-H-Si inhibits α -glucosidase via a non-competitive inhibition mechanism. The inhibition constant for MT-C3-H-Si was calculated as $9.45 \pm 1.45 \mu\text{M}$.



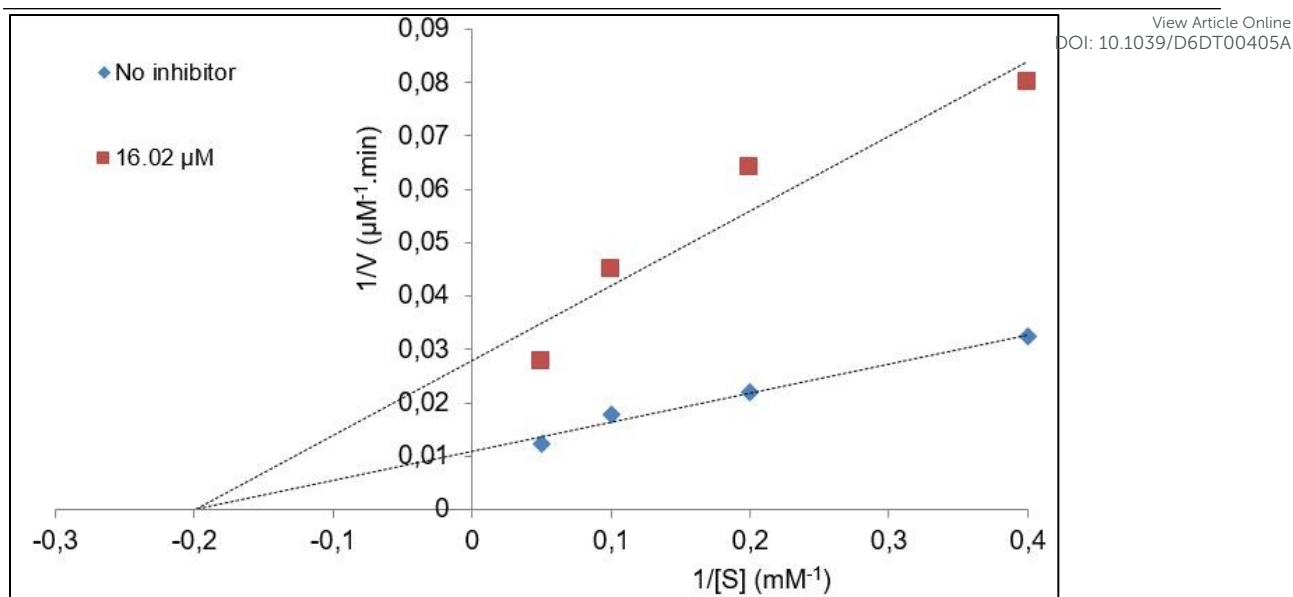


Figure 6. Lineweaver-Burk graph of MT-C3-H-Si on α -glucosidase.

Similarly, as illustrated in Fig. 7, the addition of MT-C3-D-Si resulted in a reduction of the V_m value without affecting the K_m value, demonstrating a non-competitive inhibition pattern toward α -glucosidase. The calculated K_i value for MT-C3-D-Si was $29.06 \pm 5.16 \mu\text{M}$, indicating a lower binding affinity compared to MT-C3-H-Si.

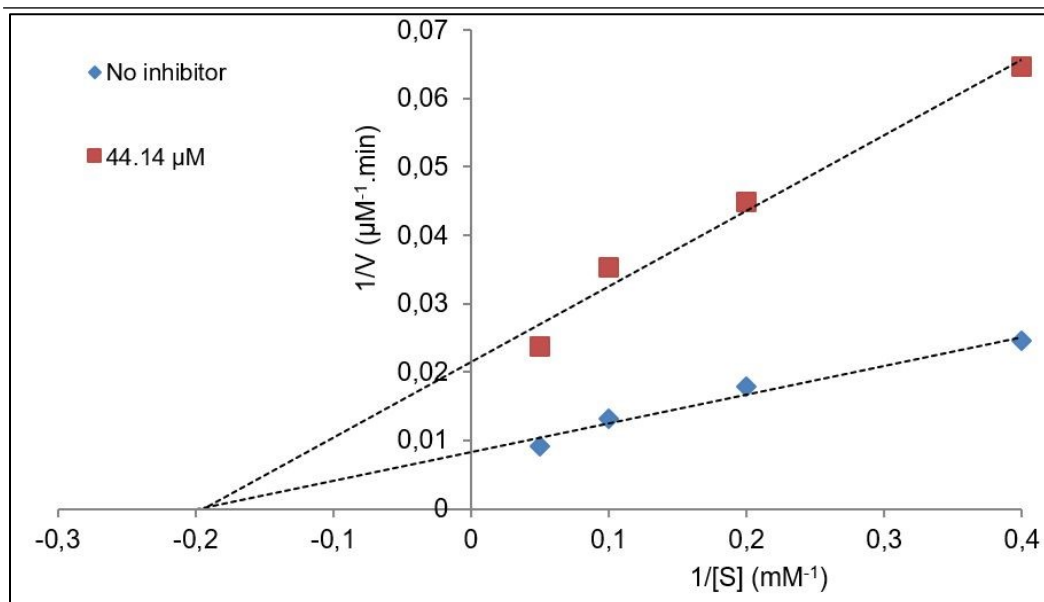


Figure 7. Lineweaver-Burk graph of MT-C3-D-Si on α -glucosidase.

The kinetic evaluation of MT-C3-H-Si and MT-C3-D-Si provided important insights into the inhibition behavior of these silicon(IV) phthalocyanines toward α -glucosidase. The observed



decrease in V_{max} without a significant change in K_m values clearly indicates a non-competitive inhibition mechanism, suggesting that both compounds interact with the enzyme at a site distinct from the active site. This behavior implies that enzyme inhibition is not directly influenced by substrate concentration and cannot be overcome by increasing substrate levels.

The non-competitive inhibition profile observed for MT-C3-H-Si and MT-C3-D-Si may be attributed to the structural features of axially disubstituted silicon(IV) phthalocyanines. The rigid macrocyclic framework and axial substitution pattern are likely to facilitate interactions with allosteric regions of the enzyme, leading to conformational changes that reduce catalytic efficiency. Such an inhibition mechanism is particularly advantageous for therapeutic applications, as it may provide more consistent enzyme inhibition under varying physiological substrate concentrations³⁹.

Comparison of the inhibition constants further reveals that MT-C3-H-Si exhibits a stronger affinity toward α -glycosidase than MT-C3-D-Si, as evidenced by its lower K_i value. This difference may be associated with variations in axial substituent architecture, which can influence molecular flexibility, steric accessibility, and the overall interaction strength with the enzyme surface^{40,41}. These findings suggest that subtle modifications in axial functionalization play a critical role in modulating enzyme–inhibitor interactions.

From a pharmacological perspective, the combination of strong α -glucosidase inhibition, limited α -amylase inhibition, and a non-competitive inhibition mechanism is highly desirable for the management of Type 2 diabetes⁴². This inhibition profile may help reduce postprandial glucose levels while minimizing gastrointestinal side effects commonly associated with strong α -amylase inhibition. Overall, the kinetic behavior of the synthesized silicon(IV) phthalocyanines supports their potential as promising candidates for further development as antidiabetic agents.

4. Conclusion

In this study, a series of axially disubstituted silicon(IV) phthalocyanines and water-soluble derivatives were synthesized and comprehensively characterized using spectroscopic techniques. The *in vitro* biological evaluation demonstrated that selected silicon(IV) phthalocyanines exhibited significant inhibitory activity against α -glycosidase, while showing comparatively weak inhibition toward α -amylase. This selective inhibition profile is considered advantageous for the management of Type 2 DM, as strong α -glycosidase inhibition combined with limited α -amylase inhibition may help reduce postprandial hyperglycemia while minimizing gastrointestinal side effects. Enzyme kinetic studies revealed that the most active



compounds, MT-C3-H-Si and MT-C3-D-Si, inhibited α -glycosidase through a non-competitive mechanism. Overall, the results of this study highlight that combination of selective enzyme inhibition and a non-competitive inhibition mechanism underscores the potential of these compounds for further pharmacological investigation. Future studies focusing on structure optimization, in silico modeling, and advanced biological evaluations may further clarify the therapeutic potential of this class of compounds in Type 2 DM management.

View Article Online
DOI: 10.1039/D6DT00405A

Author contributions

Turgut Keleş: Investigation, Methodology, Data curation.

Zekeriya Biyiklioglu: Conceptualization, Supervision, , Writing – review & editing.

Gökçe Seyhan: Investigation, Data curation, Formal analysis.

Burak Barut: Formal analysis, Writing – original draft.

Conflicts of interest

There are no conflicts to declare.

Acknowledgments

This work was supported by The Scientific and Technological Research Council of Turkey (TÜBİTAK) under Project No. 124Z983.



References

- 1 A. Poznyak, A. V. Grechko, P. Poggio, V. A. Myasoedova, V. Alfieri and A. N. Orekhov, *Int. J. Mol. Sci.*, 2020, **21**, 1–13.
- 2 M. Su, T. Tang, W. Tang, Y. Long, L. Wang and M. Liu, *Front. Immunol.*, 2023, **14**, 1–12.
- 3 W. Mi, Y. Xia and Y. Bian, *Inflamm. Res.*, 2019, **68**, 275–284.
- 4 M. J. Hossain, M. Al-Mamun and M. R. Islam, *Heal. Sci. Reports*, 2024, **7**, 5–9.
- 5 X. Cheng, J. Huang, H. Li, D. Zhao, Z. Liu, L. Zhu, Z. Zhang and W. Peng, *Phytomedicine*, 2024, **126**, 154887.
- 6 C. Ge, Z. Shi, J. He, X. Feng, K. Shang, X. Liao, Y. Liu, Y. Jiang and S. Liu, *Pharm. Biol.*, 2026, **64**, 130–142.
- 7 L. Zhao, S. Luo, Z. Peng and G. Wang, *Int. J. Biol. Macromol.*, 2025, **302**, 140637.
- 8 T. S. Chaithanya and V. Sabareesh, *Pept. Sci.*, DOI:10.1002/pep2.70017.
- 9 G. Wu, W. He, H. Rao, L. Lu, X. He and X. Hou, *Front. Endocrinol. (Lausanne)*, 2025, **16**, 1–8.
- 10 F. Khan, S. Ahmad, K. Osama, A. Farooqui, A. Kumar and S. Akhtar, *Mol. Divers.*, DOI:10.1007/s11030-025-11307-2.
- 11 Y. C. Feng, X. Wang and D. Wang, *Mater. Chem. Front.*, 2023, **8**, 228–247.
- 12 H. Y. Yenilmez, Ö. Budak, N. F. Öztürk, A. Koca, A. Boz, B. Ustamehmetoğlu and Z. Altuntaş Bayır, *Dalt. Trans.*, 2023, **53**, 1766–1778.
- 13 Ö. Güleç, A. T. Bilgiçli, C. Hepokur, A. Günsel, M. Arslan and M. Nilüfer Yarasir, *J. Photochem. Photobiol. A Chem.*, DOI:10.1016/j.jphotochem.2024.115587.
- 14 G. Zanotti, P. Imperatori, A. M. Paoletti and G. Pennesi, *Molecules*, DOI:10.3390/molecules26061760.
- 15 V. T. Verdree, S. Pakhomov, G. Su, M. W. Allen, A. C. Countryman, R. P. Hammer and S. A. Soper, *J. Fluoresc.*, 2007, **17**, 547–563.
- 16 S. Ünlü, Z. Köksal, K. Kübra Kırboğa and F. T. Elmalı, *J. Mol. Struct.*, DOI:10.1016/j.molstruc.2025.144615.
- 17 H. Messaoudi, G. Yaşa Atmaca and A. Erdoğmuş, *J. Mol. Struct.*, DOI:10.1016/j.molstruc.2024.138394.
- 18 P. Saha, S. Das, H. K. Indurthi and D. K. Sharma, *Dye. Pigment.*, 2022, **206**, 110608.
- 19 D. Li, S. Cai, P. Wang, H. Cheng, B. Cheng, Y. Zhang and G. Liu, *Adv. Healthc. Mater.*, 2023, **12**, 1–24.
- 20 D. Güngördü Solğun, S. Özdemir, A. Dündar and M. S. Ağırtaş, *J. Photochem.*



- Photobiol. A Chem.*, DOI:10.1016/j.jphotochem.2024.115794.
- 21 F. Çelik, Y. Ünver, F. OzTuncay, U. Cakmak, Y. Kolcuoglu, K. K. Uzun, H. Ozturk, N. Yorulmaz and İ. Değirmencioğlu, *J. Organomet. Chem.*, DOI:10.1016/j.jorganchem.2024.123237.
- 22 H. Yalazan, B. Barut, C. Ö. Yalçın, H. Kantekin and S. Yıldırımış, *Inorg. Chem. Commun.*, DOI:10.1016/j.inoche.2024.112548.
- 23 H. O. Gulcan, S. Unlu, I. Esiringu, T. Ercetin, Y. Sahin, D. Oz and M. F. Sahin, *Bioorganic Med. Chem.*, 2014, **22**, 5141–5154.
- 24 H. Nara, A. Kaieda, K. Sato, T. Naito, H. Mototani, H. Oki, Y. Yamamoto, H. Kuno, T. Santou, N. Kanzaki, J. Terauchi, O. Uchikawa and M. Kori, *J. Med. Chem.*, 2017, **60**, 608–626.
- 25 K. K. Palaniappan, A. A. Pitcher, B. P. Smart, D. R. Spiciarich, A. T. Iavarone and C. R. Bertozzi, *ACS Chem. Biol.*, 2011, **6**, 829–836.
- 26 T. Keles, G. Seyhan, Z. Biyiklioglu, K. Kolci, R. Reis and B. Barut, *Appl. Organomet. Chem.*, 2024, **38**, 2–9.
- 27 G. De La Torre, C. G. Claessens and T. Torres, *Chem. Commun.*, 2007, 2000–2015.
- 28 T. Nyokong, *Coord. Chem. Rev.*, 2007, **251**, 1707–1722.
- 29 B. Barut and Ü. Demirbaş, *J. Organomet. Chem.*, DOI:10.1016/j.jorganchem.2020.121423.
- 30 I. A. Khan, F. A. Saddique, S. Aslam, U. A. Ashfaq, M. Ahmad, S. A. Al-Hussain and M. E. A. Zaki, *Molecules*, 2022, **27**, 1–13.
- 31 E. Menteşe, N. Baltaş and M. Emirik, *Bioorg. Chem.*, 2020, **101**, 104002.
- 32 O. Çakmak, S. Ökten, D. Alımlı, C. C. Ersanlı, P. Taslimi and Ü. M. Koçyiğit, *J. Mol. Struct.*, DOI:10.1016/j.molstruc.2020.128666.
- 33 D. Zolotareva, A. Zazybin, A. Dauletbaev, Y. Belyankova, B. Giner Parache, S. Tursynbek, T. Seilkhanov and A. Kairullinova, *Molecules*, DOI:10.3390/molecules29133043.
- 34 L. A. Kayukova, A. B. Uzakova, G. P. Baitursynova, G. T. Dyusembaeva, Z. T. Shul'gau, A. E. Gulyaev and S. D. Sergazy, *Pharm. Chem. J.*, 2019, **53**, 129–133.
- 35 B. Saroha, G. Kumar, P. Arya, N. Raghav and S. Kumar, *Bioorg. Chem.*, 2023, **140**, 106805.
- 36 E. Tugba Saka, U. Cakmak, C. Akkol and Z. Biyiklioglu, *Polyhedron*, 2023, **243**, 116522.
- 37 M. A. Huneif, D. B. Alshehri, K. S. Alshaibari, M. Z. Dammaj, M. H. Mahnashi, S. U.

View Article Online
DOI: 10.1039/D6DT00405A



Majid, M. A. Javed, S. Ahmad, U. Rashid and A. Sadiq, *Biomed. Pharmacother.*, 2022, **150**, 113038. Article Online
DOI: 10.1039/D6DT00405A

- 38 M. Askarzadeh, H. Azizian, M. Adib, M. Mohammadi-Khanaposhtani, S. Mojtavavi, M. A. Faramarzi, S. M. Sajjadi-Jazi, B. Larijani, H. Hamedifar and M. Mahdavi, *Sci. Rep.*, 2022, **12**, 1–16.
- 39 S. N. Meena, U. kumar, M. M. Naik, S. C. Ghadi and S. G. Tilve, *Bioorganic Med. Chem.*, 2019, **27**, 2340–2344.
- 40 E. Güzel, B. S. Arslan, K. Çlkrkçl, A. Ergün, N. Gençer, O. Arslan, I. Şişman and M. Nebioğlu, *J. Porphyr. Phthalocyanines*, 2020, **24**, 1047–1053.
- 41 T. Keleş, Z. Biyiklioglu, E. Gültekin and O. Bekircan, *Inorganica Chim. Acta*, 2019, **487**, 201–207.
- 42 S. Rocha, A. Sousa, D. Ribeiro, C. M. Correia, V. L. M. Silva, C. M. M. Santos, A. M. S. Silva, A. N. Araújo, E. Fernandes and M. Freitas, *Food Funct.*, 2019, **10**, 5510–5520.

References 43-46 are cited in the Supplementary information (SI).



View Article Online
DOI: 10.1039/D6DT00405A

- The data supporting this article have been included as part of the Supplementary Information.

